BIOCHEMISTRY

 Volume 46, Number 43 October 30, 2007

Accelerated Publications

Mutation of Arginine 357 of the CP43 Protein of Photosystem II Severely Impairs the Catalytic S-State Cycle of the H_2O Oxidation Complex†

Hong Jin Hwang,‡ Preston Dilbeck,‡ Richard J. Debus,§ and Robert L. Burnap*,‡

Department of Microbiology and Molecular Genetics, Oklahoma State University, Stillwater, Oklahoma 74078, and Department of Biochemistry, University of California, Riverside, California 92521

Received July 13, 2007; Revised Manuscript Received September 9, 2007

ABSTRACT: Basic amino acid side chains situated in active sites may mediate critical proton transfers during an enzymatic catalytic cycle. In the case of photosynthetic water oxidation, a strong base is postulated to facilitate the deprotonation of the active site Mn_4-Ca cluster, thereby allowing the otherwise thermodynamically constrained transfer of an electron away from the Mn_4-Ca cluster to the oxidized redox active tyrosine radical, $Y_Z^{\bullet}$, generated by photosynthetic charge separation. Arginine 357 of the CP43 polypeptide may be located in the second coordination shell of the O_2-evolving Mn_4-Ca cluster of photosystem II (PSII) according to current structural models. An ostensibly conservative substitution mutation, CP43-357K, was investigated using polarographic and fluorescence techniques in evaluating its potential impact on S-state cycling. Cells containing the CP43-357K mutation lost their capacity for autotrophic growth and exhibited a drastic reduction in O_2 evolving activity (~15% of that of the wild type) despite the fact that mutant cells contained more than 80% of the concentration of charge-separating PSII reaction centers and more than half of these contained photooxidizable Mn. Fluorescence kinetics indicated that acceptor side electron transfer, dominated by the transfer of electrons from Q_A^- to Q_B, was unaffected, but the fraction of centers containing Mn clusters capable of forming the S_2 state was reduced to ~40% of that of the wild type. Analysis of O_2 yields using a bare platinum electrode indicated a severe defect in the S-state cycling properties of the mutant H_2O oxidation complexes. Although O_2 evolution was delayed to the third flash during a train of single-turnover saturating flashes, the pattern of O_2 emission did not exhibit a discernible periodicity indicating a very high miss factor, which was estimated to be ~45% compared to the wild-type value of ~10%. On the other hand, the multiflash fluorescence measurements indicate that the yield of formation of the S_2 state from S_1 is diminished by ~20%, although this latter estimate is complicated by the presence of damaged PSII centers. Taken together, the experiments indicate that the high miss factor observed during S-state cycling is likely due to a defect in the higher S-state transitions. These results are discussed in relation to the idea that CP43-R357 may serve as a ligand to bicarbonate or as the catalytic base proposed to mediate proton-coupled electron transfer (PCET) in the higher S states of the catalytic cycle of H_2O oxidation.

The light-driven extraction of hydrogen atoms from substrate water molecules is the signature catalytic feature of oxygenic photosynthesis and is catalyzed by the H_2O oxidation complex (WOC)[1] of photosystem II (PSII). This thermodynamically difficult process is further complicated by the fact that the full oxidation of water, with the concomitant liberation of molecular oxygen, is a four-electron, four-proton process, whereas oxidizing power produced at the photochemical reaction center is univalent, occurring one electron per charge separation. On the basis

† This work was funded by the National Science Foundation (Grant MCB-0448567 to R.L.B.) and the National Institutes of Health (Grant GM-076232 to R.J.D.).

* To whom correspondence should be addressed. Phone: (405) 744-7445. Fax: (405) 744-6790. E-mail: burnap@biochem.okstate.edu.

‡ Oklahoma State University.

§ University of California.

10.1021/bi701387b CCC: $37.00
Published on Web 10/04/2007

of the observation that the yield of oxygen oscillates with a periodicity of 4 when dark-adapted samples are exposed to a train of brief (<10 μs) saturating flashes (*1*), Kok and coworkers developed a model of the catalytic cycle involving the sequential accumulation of four oxidizing equivalents prior to the release of dioxygen (*2*). The catalytic cycle of the H_2O oxidation complex most basically consists of a sequence of oxidation states, termed S states, designated S_0−S_4. The S_1 state predominates in dark-adapted samples, accounting for maximal yields occurring on the third flash, the S_4 state being a hypothesized transient state preceding dioxygen bond formation. A metal cluster consisting of four Mn molecules and one Ca (Mn_4−Ca) is involved in this accumulation of oxidizing equivalents due to light-induced electron transfer reactions within PSII (for reviews, see refs *3*−*6*).

The three-dimensional structure of the *Thermosynechococcus elongatus* PSII complex has been determined up to 3.0 Å resolution (*7*−*10*) using X-ray diffraction, although the likelihood of radiation damage to Mn_4−Ca during data collection has raised questions about the actual structure of Mn_4−Ca (*11*−*13*). The cofactors involved in light-induced primary charge separation in the PSII reaction center are coordinated by the hetrodimeric D1 and D2 polypeptides, including the primary electron donor, P680, and the early acceptor, $Pheo_{D1}$, a pheophytin, and plastoquinone secondary acceptors, Q_A and Q_B (reviewed in ref *14*). The D1−D2 heterodimer is surrounded by a number of intrinsic and extrinsic polypeptides, most notably for this discussion, the CP43 and CP47 chlorophyll proteins, which serve as proximal light-harvesting antennae to the reaction center and, in the case of CP43, provide key amino acid side chains to the active site of the WOC (see below). Photochemical charge separation involves the rapid formation of the $P680^+Pheo_{D1}^-$ radical pair with the subsequent transfer of the electron from $Pheo_{D1}^-$ to the nonexchangeable plastoquinone, Q_A^-, all occurring in <1 μs. The charge-separated state is further stabilized when Q_A^- transfers its electron to an exchangeable plastoquinone Q_B, which occurs on a time scale of hundreds of microseconds. In its doubly reduced and protonated form, this plastoquinone diffuses from the Q_B binding site into the lipid bilayer to interact with, and become oxidized by, the remainder of the electron transport chain. Photooxidized primary donor, $P680^+$, is re-reduced in <1 μs by the redox active tyrosine, Y_Z, of the D1 protein. Y_Z forms the interface between the four-oxidizing equivalent accumulating capacity of Mn_4−Ca and the univalent oxidizing power of the photochemical reaction center (*15*).

One of the important findings of the recent X-ray crystallographic analyses of the *Thermosynechococcus* PSII reaction centers was the identification of residues participating in the formation of the WOC that are part of the large lumenal e-loop connecting transmembrane helices 5 and 6 of CP43.

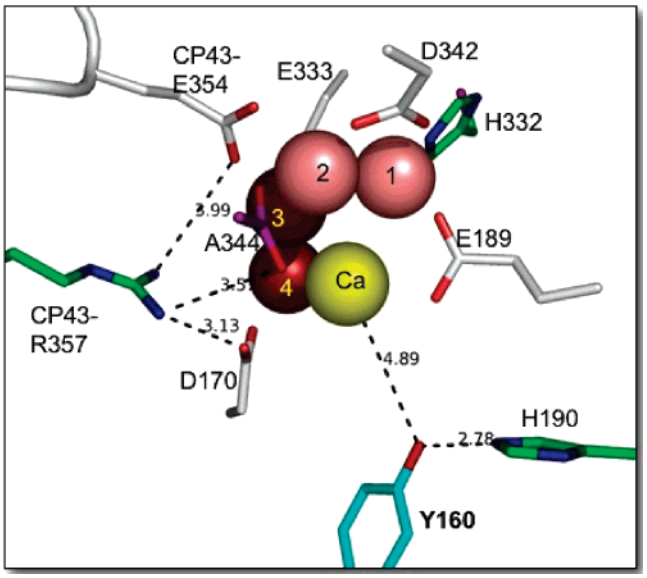

FIGURE 1: CP43-Arg357 environment within the PSII H_2O oxidation complex. Red circles with numbers represent the four Mn atoms of the cluster (but see ref *11*). The image was made using the coordinates deposited in the Protein Data Bank (2AXT) by Loll et al. (*9*). Dashed lines indicate distances in angstroms. Note that the CP43-Arg357 guanidinium N atom is ~3 Å from the carboxylate O atom of high-affinity Mn site residue D1-Asp170 and ~3.5 Å from the mature D1 terminal carboxyl moiety essential for the formation of the metal cluster.

These findings are consistent with earlier site-directed mutagenesis studies that had highlighted the functional importance of basic and acidic residues located within the CP43 e-loop (*16*, *17*). According to current structural models, coordination of Mn_4−Ca involves several amino acids of the D1 polypeptide as well as glutamate 354 of the CP43 polypeptide (CP43-E354). These assignments, however, need to be treated with due caution because (1) the resolution of the crystallographic data remains above 3 Å and (2) the above-mentioned damage to Mn_4−Ca (*11*−*13*) is likely to cause dislocations of the amino acid ligands as well as the cluster itself. Nevertheless, ligation of Mn by CP43-E354 is consistent with the observation that the mutation of the equivalent residue to glutamine (CP43-E354Q)[2] in the genetic model, *Synechocystis* sp. PCC6803, results in severely impaired O_2 evolving activity (*17*). Nearby, in the second coordination sphere of Mn_4−Ca in the structure models, is arginine 357 (CP43-R357), which has been strictly conserved during the evolution of PSII, suggesting an important function within the WOC (*18*). As shown in Figure 1, the model of Loll et al. (*9*) places the guanidinium N atom of CP43-Arg357 approximately 3 Å from the carboxylate O atom of D1-Asp170, the critical high-affinity site residue. Indeed, mutation of this residue to a serine (CP43-R357S) results in a severe decrease in O_2 evolving activity (*16*),

[1] Abbreviations: CP43, chlorophyll protein subunit of the PSII complex encoded by the *psbC* gene; D1, reaction center protein encoded by the *psbA* gene; DCBQ, 2,6-dichlorobenzoquinone; EDTA, (ethylenedinitrilo)tetraacetic acid; Hepes, 4-(2-hydroxyethyl)-1-piperazineethanesulfonic acid; HBG-11, normal BG-11 growth medium buffered with Hepes-NaOH (pH 8); LED, light-emitting diode; Mn_4−Ca, metal cluster functioning in H_2O oxidation; PCET, proton-coupled electron transfer; PSII, photosystem II; WOC, H_2O oxidation complex of PSII; XRD, X-ray diffraction; Y_Z, redox active tyrosine of the D1 protein acting as a secondary electron donor of the reaction center.

[2] Because of differences in the length and numbering of the amino acid sequence of the CP43 protein structurally resolved from *Thermosynechoccus* PSII and CP43 found in the genetic model *Synechocystis* sp. PCC6803, the amino acid sequence number designations of structural equivalent amino acids do not match. The designations of *Thermosynechoccus* CP43 will be used for the mutations at the equivalent positions in *Synechocystis* strains used in this study. Specifically, the CP43-E354 and CP43-R357 nomenclature of the three-dimensional structure has been used for the mutant strains with CP43-E339 and CP43-R342 substitutions of the *Synechocystis* strains used here.

including a marked increase in the miss factor (*19*). This arginine was proposed to coordinate a bicarbonate anion near Mn_4−Ca and be responsible for the activation of its assembly and catalytic activity (*19*−*21*). In principle, the binding of the bicarbonate anion to CP43-R357 could also provide an alternate means of ligating a metal atom of Mn_4−Ca considering that in the transferrin family of Fe-binding proteins, a strongly conserved arginine mediates the binding of the transition metal by binding and positioning a bicarbonate anion, which, in turn, acts one of the direct ligands to the coordinated Fe (*22*). Alternatively, CP43-R357 may mediate chloride binding, consistent with recent EXAFS results (*23*) and the hypothesis that the anion is involved in the positioning of substrate water. Finally, CP43-R357 has been proposed to serve as a catalytic base functioning to extract protons directly from substrate water (*24*, *25*). The action of such a catalytic base was originally predicted by Krishtalik, considering the relatively small driving force associated with the oxidation of H_2O by $P680^+$ (*26*). Time-resolved X-ray studies monitoring the redox state of Mn_4−Ca revealed a 200 μs lag initiating the O_2-yielding S_3−$[S_4]$−S_0 transition (*24*). The lag was discussed in terms of a deprotonation of a catalytic base, perhaps CP43-R357, with the actual loss of the proton being the electrostatic result of the positive charge developing in the vicinity of Y_Z due to its oxidation by $P680^+$. CP43-R357 also figures in related arguments concerning whether electron transfer is coupled to proton transfer [proton-coupled electron transfer (PCET)], where it is suggested that Mn oxidation during the S_2−S_3 and S_3−S_0 transitions, but not the S_0−S_1 and S_1−S_2 transitions, requires deprotonation of a Mn_4−Ca proximal base (mix-mode PCET) (*24*, *25*, *27*). In this report, we further investigate the role of CP43 position 357, analyzing the lysine substitution mutation, CP43-357K, using polarographic and fluorescence techniques. In the case of the bicarbonate-coordinating arginine found in transferrins, substitutions with lysine are tolerated, and the mutant is able to bind iron, although release of iron is moderately faster (*28*). Although the substitution of the arginine with a lysine is apparently a more conservative mutation than the serine substitution, its effect appears to be as severe as that of the previously investigated CP43-R357S (*16*, *19*). Analysis of the mutant S-state cycling characteristics shows that while the mutation is likely to have a strong impact on the ability of Mn_4−Ca to advance through the higher S states, the transition probability of the S_1−S_2 transition is already deeply impaired.

MATERIALS AND METHODS

Strains and Growth Conditions. The naturally transformable, glucose-utilizing strain of *Synechocystis* sp. PCC6803 and the mutant derivatives were maintained on solid agar and in liquid BG-11 medium buffered with 20 mM HEPES-NaOH (pH 8.0) (HBG-11) supplemented with 5 mM glucose and 10 μM DCMU (*29*−*34*). Experimental cultures were grown in HBG-11 with 5 mM glucose and under a PFD (photon flux density) of ~70 μmol m^{-2} s^{-1} at 30 °C with bubbling with filter-sterilized air enriched with 3% CO_2. Light intensity measurements were made with a LiCor (Lincoln, NE) sensor. The CP43-R357K mutation was constructed in the *psbC* gene and transformed into a host strain of *Synechocystis* that lacks the large extrinsic loop of CP43 and contains a hexahistidine tag (His tag) fused to the C-terminus of CP47 (*35*). Construction of mutations in the large extrinsic loop of CP43 is similar to that described previously (*36*). The similarly hexahistidine-tagged strain designated HT-3 (*37*) is identical to the wild type, apart from the His tag on CP47, and has kinetic properties indistinguishable from those of the wild type (*38*). It was also noticed that liquid cultures of CP43-R357K exhibited considerable variability in the content of PSII (assayed as variable fluorescence) depending upon the age of the culture and the fact that the highest PSII activities were obtained from mid-log phase cultures (OD_{750} ~ 1.2). All preparations were therefore obtained from cells harvested during this phase.

Isolation of Thylakoid Membranes. Thylakoid membranes were isolated using previously described procedures (*29*, *30*, *32*, *33*). Harvested cells were pelleted by centrifugation (5 min at 8000*g*), suspended in a buffer containing 50 mM MES-NaOH (pH 6.0), 1.2 M betaine, 10% (v/v) glycerol, 5 mM $CaCl_2$, 5 mM $MgCl_2$, 1 mM benzamidine, 1 mM ϵ-amino-*n*-caproic acid, 1 mM phenylmethanesulfonyl fluoride, and then broken by nine cycles (10 s on and 5 min off) in a glass bead homogenizer (Bead-Beater, BioSpec Products, Bartlesville, OK). Unbroken cells and debris were removed by centrifugation, and the supernatant material containing thylakoid membranes was centrifuged (20 min at 40 000 rpm in a Beckman 70Ti rotor) to collect the thylakoids, which were then resuspended to a concentration of 1.0−1.5 mg of Chl/mL in a buffer containing 50 mM MES-NaOH (pH 6.0), 1.2 M betaine, 10% (v/v) glycerol, 20 mM $CaCl_2$, and 5 mM $MgCl_2$. The concentrated thylakoid membranes were flash-frozen as 0.5 mL aliquots in liquid nitrogen and stored at −80 °C until they were used.

Flash O_2 Yield and Kinetic Measurements. Flash O_2 yields were performed using a bare platinum electrode that permits the centrifugal deposition of samples upon the electrode surface (*39*), as described previously (*31*, *40*). For each measurement, membrane samples containing 2 μg of Chl in 400 μL of a buffer consisting of 50 mM MES-NaOH, 10 mM $CaCl_2$, 5 mM $MgCl_2$, and 800 mM sucrose (pH 6.5) were centrifugally deposited at 16400*g* for 10 min onto the platinum surface of the electrode in a Sorvall HB-4 swing-out rotor. The buffer was supplemented with 250 mM NaCl to increase the electrical conductivity to better resolve the rise kinetic corresponding to oxygen release during the S_0−$[S_4]$−S_0 transition in experiments attempting to resolve the dioxygen release kinetics and 100 mM NaCl for experiments focusing on flash yield patterns in dark-adapted samples. Samples were generally given a sequence of 20 saturating xenon preflashes (6 μs, full width at half-maximal intensity) and then dark-adapted for 10 min prior to the initiation of the measurement of O_2 signals in response to a train of saturating xenon flashes. For some experiments, samples were extensively dark adapted (>2 h) as indicated in the text. Polarization of the electrode (0.73 V) was initiated 20 s before the initiation of data acquisition (10 points per ms), and the flash sequence (19 flashes at a frequency of 4 Hz) was initiated 333 ms after that. The polarographic amplifier response time is approximately 100 μs. Timing of the flash points relative to the O_2 signals and instrument response time was verified by separate trials by allowing exposure of the silver electrode and using the photoelectric signal resulting from the xenon flash impinging it. Analysis of the oscillatory pattern of release of O_2 from dark-adapted samples subject

Table 1: Characterization of Wild-Type and CP43-R357K Mutant *Synechocystis* sp. PCC6803[a]

strain	oxygen evolution[b] [μmol of $O_2^{\bullet}$ (mg of Chl)$^{-1}$ h^{-1} (% of wt)]		relative PSII content assayed as the maximum variable fluorescence[c] (% of wt)	fraction of PSII centers containing photooxidizable Mn[d]
	cells	membranes		
wild type	710 (100)	690 (100)	0.72 (100)	>98%
CP43-R357K	130 (18)	110 (15)	0.59 (82)	58%

[a] All the data are the average of three or more measurements, and standard deviations do not exceed 10%. [b] Oxygen evolution in cells was assessed at a chlorophyll concentration of 6.25 μg/mL in HN buffer [10 mM Hepes-NaOH and 30 mM NaCl (pH 7.2)] with the addition of 750 μM DCBQ and 2 mM $K_3Fe(CN)_6$. Rates of membranes were measured in a buffer consisting of 50 mM MES-NaOH, 10 mM $CaCl_2$, 5 mM $MgCl_2$, and 800 mM sucrose (pH 6.5). [c] The relative PSII content was estimated from the yield of variable chlorophyll *a* fluorescence $(F_{max} - F_0)/F_0$. Measurements were taken in the presence of 20 mM hydroxylamine and 20 μM DCMU, according to the methods of Nixon and Diner (*39*) and Chu et al. (*46*). [d] Estimated from the rate of accumulation of Q_A^- under strong illumination and in the presence of DCMU (*46*).

to a train of flashes was performed assuming a four-state model (*35*, *41*−*43*). To obtain better a signal-to-noise ratio for analysis of the rise kinetic due to oxygen release during the $S_0-[S_4]-S_0$ transition, 40 individual signals were averaged.

Quantification of PSII and Measurements of Fluorescence Kinetics. Measurements of variable fluorescence yields were performed with a double-modulation kinetic chlorophyll fluorometer fitted with a second actinic flash illumination source (PSI Instruments, Brno, Czech Republic). Cells from the mid-log growth phase were kept under dim light on a shaker at 200 rpm before being used for experiments and diluted to 5 μg of Chl/mL for measurements. Fluorescence kinetics were assayed using variations of the standard instrument settings that sample the low-fluorescence F_0 state in dark-adapted samples by probing fluorescence yield with four measuring pulses followed 200 μs later by a 30 μs saturating actinic flash, followed by a sequence of measuring pulses beginning 50 μs after the actinic flash. PSII has a high fluorescent yield when it is in the $P680Q_A^-$ state, which is formed when P680 absorbs a photon of light and donates an electron to Q_A. Without inhibitors, the principal component of decay of this state is due to the oxidation of Q_A^- by a plastoquinone in the Q_B site. When DCMU blocks the transfer of electrons from Q_A^- to Q_B, this causes P680 Q_A^- to persist until the electron recombines with oxidants on the donor side, which in the case of the intact enzyme is principally the S_2 state of Mn_4-Ca. The total variable fluorescence was evaluated with the relation $F_v = (F_t - F_0)/F_0$, where F_t is the fluorescence at time t and F_0 is the lowest level of fluorescence yield obtained as the average yield of a sequence of four weak measuring flashes applied before the first saturating flash. Analysis of the kinetic components of the fluorescence decay was performed according to ref *44* except that a correction for exciton sharing between centers was not applied (*44*, *45*). However, the flashes were oversaturating, helping to ensure all centers advanced in multiflash experiments, but this resulted in a relative increase in the observed rates of decay (*45*).

Estimation of the concentration of charge-separating PSII centers was performed essentially as described previously (*39*, *46*). The cells were incubated in the dark for 5 min with 300 μM DCBQ and 300 μM KFeCN to oxidize any residual Q_A^-. DCMU was then added to a concentration of 20 μM and the mixture allowed to incubate for 1 min, and then 10 mM hydroxylamine was added. Measurement of variable fluorescence was initiated several seconds after the hydroxylamine was added by applying 30 saturating actinic flashes (20 Hz), with the fluorescence yield being sampled after each flash.

RESULTS

Growth and Oxygen Evolution Characteristics. The function of strictly conserved (*18*) CP43-R357 was explored by the construction and analysis of the ostensibly conservative Arg to Lys substitution, CP43-R357K. While this mutation was hypothesized to provide an intermediate impact upon H_2O oxidation activity compared to the CP43-R357S (*16*) mutant and the wild type, the Arg to Lys substitution actually proved to have an impact nearly as severe as that of the chemically more disparate Arg to Ser substitution (*16*, *19*). Like the CP43-R357S cells, CP43-R357K cells were incapable of autotrophic growth, and the light-saturated, steady-state O_2 evolving activity of CP43-R357K cells was highly depressed. Additions of higher concentrations of chloride and calcium in the culture medium did not restore the capacity for autotrophic growth. Maximal rates of O_2 evolution were approximately 130 μmol of O_2 (mg of Chl)$^{-1}$ h^{-1} for CP43-R357K compared to 710 μmol of O_2 (μg of Chl)$^{-1}$ h^{-1} for wild-type cells grown under similar conditions (Table 1). The disparity between the wild type and the mutant was somewhat greater in isolated membranes, indicating the mutation causes a slight decrease in stability, presumably of the WOC, during preparation of the membranes.

To evaluate whether this severe depression in the maximal rate of O_2 evolution corresponded to a decline in the cellular content of PSII, the fraction of charge-separating PSII centers relative to the wild type was assayed by measuring variable fluorescence in the presence of the artificial PSII electron donor, hydroxylamine (*39*, *46*). This assay measures the relative concentration of PSII centers capable of transferring electrons from the PSII donor side to the plastoquinone at the Q_A site, and this concentration has been shown to correlate with the concentration of PSII herbicide-binding sites assayed using radiolabeled [^{14}C]DCMU (*46*). In contrast to the severe depression in the maximal rate of O_2 evolution, the content of assembled, charge-separating PSII centers was more than 80% of that of the wild type. Therefore, it is evident that the CP43-R357K mutation does not greatly weaken the ability to assemble photochemically active PSII reaction centers but instead severely impairs the capacity to sustain H_2O oxidation activity in the PSII centers that are capable of charge separation.

The fraction of charge-separating centers with bound photooxidizable Mn was estimated using an assay that relies upon the accumulation of Q_A^- during exposure to saturating

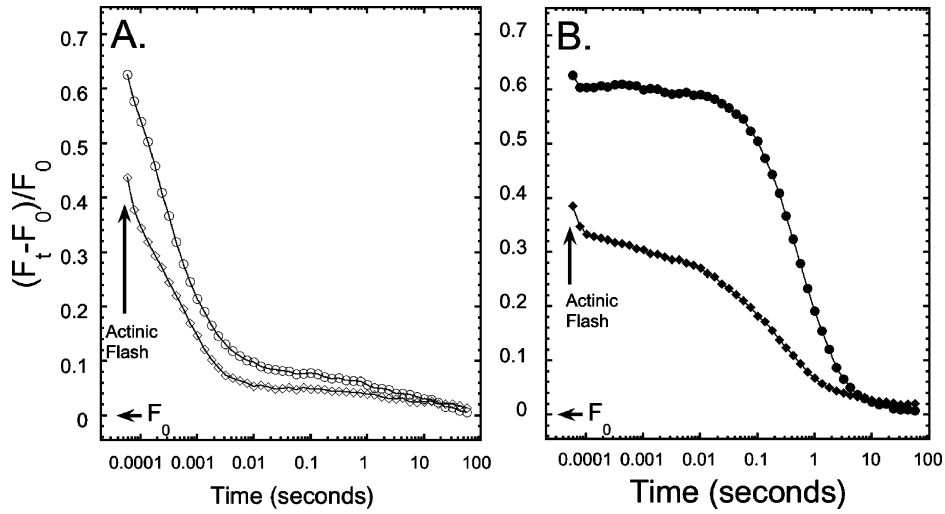

FIGURE 2: Decay of flash-induced variable fluorescence. Wild-type (circles) and CP43-R35K (diamonds) cells in the absence (A) and presence of 20 μM DCMU (B) were analyzed using a double-modulation kinetic fluorometer. Four weak measuring pulses were applied at 200 μs intervals to measure F_0, followed 200 μs later by a 30 μs saturating actinic flash. The decay of the fluorescence yield was monitored by a train of weak measuring light pulses (eight per decade of time) starting 50 μs after the saturating actinic flash. The highest fluorescence yield level corresponds to the first sampling (filled symbols in panel A) in the train of weak measuring light pulses in both samples which occurred at the first time point 50 μs after the termination of the saturating flash. Each trace represents the average of three measurements.

continuous illumination based on the principal that centers containing photooxidizable Mn will not accumulate Q_A^- as a result of donation by secondary PSII donors that compete with bound Mn for the reduction of $P680^+$ (*46*). As shown in the last column of Table 1, more than half (58%) of the charge-separating PSII centers are estimated to contain photooxidizable Mn. While this number can be considered only approximate for a variety of reasons (*46*, *47*), one can conclude that the CP43-R357K mutation causes a substantial fraction of centers to lack photooxidizable Mn in vivo, yet this fraction is probably too small to account the very low rates of O_2 evolving activity in the mutant. The relative content of charge-separating centers (~80%) and the fraction of charge-separating centers containing photooxidizable Mn (~55%) allow us to estimate that the mutant has approximately 45% of the centers with photooxidizable Mn compared to the wild type. Therefore, the low O_2 evolving activity in the mutant (<20% of that of the wild type) is probably due to either (1) a large fraction of centers with photooxidizable Mn that cannot catalyze O_2 evolution or (2) a population of centers containing assembled Mn_4−Ca but which are very impaired in terms of their intrinsic rate or quantum efficiency of catalytic turnover.

Fluorescence Measurements. To evaluate the basis of the greatly reduced steady-state H_2O oxidation activity in PSII of CP43-R357K, the properties of the electron acceptor and donor sides of the mutant reaction centers were investigated by assessing the relaxation of flash-induced variable fluorescence. Illumination of dark-adapted samples by a single saturating flash results in the rapid formation of Q_A^- and an oxidized donor side of PSII, wherein the oxidant is transferred from $P680^+$ to secondary donors, principally Y_Z and Mn_4−Ca in the intact wild-type system. The dark-adapted samples are in a low-fluorescence yield state corresponding to the Y_ZP680Q_A state. Application of a saturating actinic flash rapidly forms the low-fluorescence $Y_ZP680^+Q_A^-$ state. Due to limitations in the time resolution of the fluorescence kinetics instrument, the subsequent rapid reduction of $P680^+$ by Y_Z is not resolved and the first time point, occurring 50 μs after the saturating actinic flash, mainly captures the highly fluorescent $P680Q_A^-$ state. Consequently, this initial 50 μs sampling time point generally returns the highest fluorescence yield value of the entire kinetic trace, and the remainder of the fluorescence transient is a multicomponent decay that corresponds to the reoxidation of Q_A^- and reformation of the Y_ZP680Q_A state.

Figure 2A shows typical kinetic traces of the variable fluorescence of wild-type (○) *Synechocystis* and the mutant CP43-R357K (◇) in the absence DCMU. In the absence of DCMU, the principal pathway for reoxidation Q_A^- is the forward electron transfer to the Q_B site. While the amplitude of the maximal variable fluorescence is diminished in the mutant to 60−70% of that of the wild type in the absence of DCMU, the kinetics of decay were not discernibly altered. Therefore, it is concluded that the CP43-R357K mutation does not appreciably affect the acceptor side of PSII, consistent with the donor side location of the mutation; however, the overall lower amplitude of the signal (~70% compared to that of the wild type at the first time point after the flash) is largely due to the reduced concentration of charge-separating centers as noted above.

Significant kinetic differences between the mutant and wild type were, however, observed in the presence of DCMU where the primary avenue of Q_A^- reoxidation is recombination with the oxidant donor side. Figure 2B shows typical kinetic traces of the flash-induced variable fluorescence of wild-type (●) *Synechocystis* and the mutant CP43-R35K (◆) in the presence of DCMU. Fluorescence relaxation in the wild type is adequately described by assuming two decay components (*44*), a fast kinetic phase with a characteristic time of 1.1 ms and a slower phase with characteristic time of 450 ms, which have relative amplitudes of 3 and 97%, respectively. The predominant slower component of decay corresponds to S_2-Q_A^- charge recombination (*44*). The corresponding mutant trace exhibits kinetic features, notably a prominent fast phase, that are not obvious in the wild type

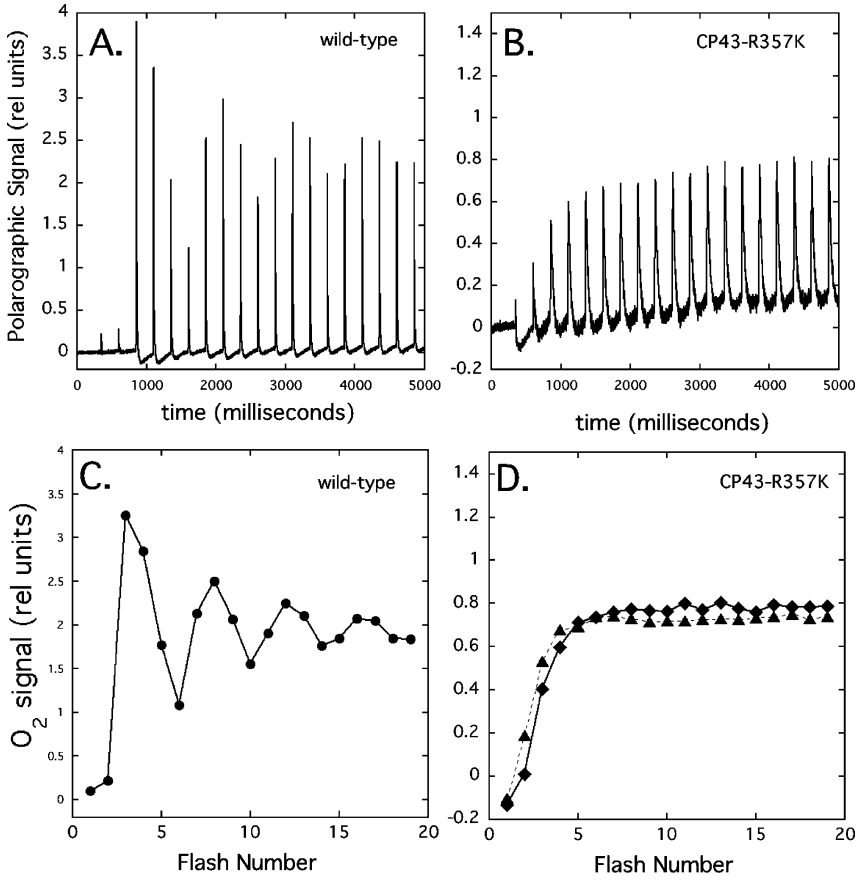

FIGURE 3: Flash O_2 yields of isolated membranes. Dark-adapted thylakoid membranes that have been centrifugally deposited upon the surface of a bare platinum electrode were given a sequence of 19 saturating xenon flashes at 4 Hz. Panels A and B are oxygen signals of mutant and wild-type membranes over 5 s. Panels C and D show an oscillatory pattern of oxygen release as a function of flash number: wild-type membranes, dark-adapted for 10 min (●); CP43-R357K, dark-adapted for 10 min (▲) or dark-adapted for 45 min (◆). After deposition on the electrode surface, membranes were given a sequence of 19 preflashes and dark-adapted for 10 min, and then the measuring flashes were applied. The gain on the polarographic signal amplifier was set to double the sensitivity for the mutant membranes because of their smaller signal amplitudes (~10% of that of the wild type on similar amplifier gain settings). Note that the unfiltered xenon flash lamp produces an artifactual photoelectric signal from the electrode, resulting in a brief upward deflection on each flash.

and indicate that the CP43-R357K mutation results in a significant modification of the donor side. Analysis of the decay curve in the mutant indicates contributions consisting of a 0.9 ms phase with a 41% relative amplitude, a 10 ms phase (13%), and a slower 370 ms (46%) phase. The prominent 0.9 and 10 ms fast phases in the mutant are likely due to rapid recombination between Q_A^- and $P680^+$ or Y_Z^+ in centers which fail to advance Mn_4−Ca to the S_2 state or which do not have a fully intact donor side, whereas the slower (370 ms) component of decay is likely to be due to S_2-Q_A^- charge recombination.

Oxygen Yield Characteristics Using a Bare Platinum Electrode. To further probe the impaired O_2 evolving activity in CP43-R357K, thylakoid membranes were isolated and analyzed using a centrifugal bare platinum electrode. The patterns of flash O_2 yield give information about the S-state cycling kinetics of the WOC and are shown in Figure 3. After deposition on the electrode surface, membranes were given a sequence of 19 preflashes, dark-adapted for 10 min, and then were illuminated by a sequence of saturating, single-turnover flashes given at a frequency of 4 Hz. The preflash sequence is given to fully oxidize centers that may populate the so-called "super-reduced" S_{-1} and S_{-2} states, while the intervening 10 min dark period allows PSII centers to relax to the S_0 and S_1 states. It is worth noting that the gain in the polarographic signal amplifier was set to twice the sensitivity for the mutant membranes for these measurements. Considering this, the amplitudes of the O_2 signals in the mutants were diminished to ~10% compared to that of the wild type, which is roughly consistent with the lower maximal rates of O_2 evolution described above. An effect due to the addition of bicarbonate reported for CP43-R357S was not observed for CP43-R357K.

The most striking aspect of the O_2 yield measurements was that the mutant does not exhibit any oscillatory pattern (Figure 3B,D). The wild type (Figure 3A,C) exhibits a deep and sustained period four oscillation in O_2 yields typical of the dark-adapted WOC (*1*, *2*, *48*). The mutant lacks these oscillations. While the first major O_2 signal in CP43-R357K, 45 min dark-adapted membranes was delayed until the third flash, its magnitude actually increased on the subsequent flashes until reaching a steady-state amplitude on the fifth and six flashes that was maintained throughout the remaining flash sequence [Figure 3D (◆)]. If samples are given 19 preflashes and dark-adapted for 10 min, a relatively small signal on the second flash in the CP43-R357K trace is observed [Figure 3D (▲)]. The small O_2 signal on the second flash is attributed to centers failing to fully decay to the S_0 and S_1 states during the intervening 10 min dark period between the preflashes and the onset of the measuring flash sequence. It indicates that either the S_2 or the S_3 state is more stable than the corresponding state(s) in the wild type, which

Table 2: S-State Decay Cycling Parameters[a]

strain	S-state distribution [$S_0/S_1/S_2/S_3$ (%)]	misses, α	hits, β	double hits, γ	deactivations, δ	O_2 signal rise[b] $t_{1/2}$, membranes
wild-type	27/69/2/2[a]	11%	84%	2%	3%	0.9 ms
CP43-R357K	27/69/2/2[c]	46%	54%	−	−	3.2 ms

[a] Cells were given a series of 20 preflashes prior to the dark period (10 min for the wild type and 20 min for CP43-R357K) preceding the series of measuring flashes. Numerical analysis of the amplitudes was performed using a four-state model as described previously (*41*, *43*). [b] Oxygen signal rise kinetics was estimated from the rising portion of the O_2 signal (Figure 4) using the exponential method as described previously (*51*). [c] The absence of discernible oscillations in the pattern of O_2 release in the CP43-R357K mutant precluded estimation of the S-state distribution by fitting; therefore, the values for the wild type were assumed to make an estimate of the miss parameter.

completely relaxes to predominantly a mixture of the centers in the S_0 and S_1 state (Table 2) during the 10 min dark period (*1*, *2*, *48*), as previously observed for similar *Synechocystis* membrane preparations (*31*, *49*). The delay in the appearance of the polarographic signals and the dark decay characteristics suggestive of a stabilized S_2 and/or S_3 state are consistent with the signals being due to O_2 rather than another species such as hydrogen peroxide. Furthermore, oxygen evolution measurements using a Clark-type concentration electrode, which excludes hydrogen peroxide from the reactive platinum surface of the electrode, showed no enhancement with the addition of catalase (not shown), suggesting that the species released by membranes under illumination truly is oxygen. On the basis of these considerations, it is also very unlikely that the gradually developing O_2 signal in CP43-R357K is due to the presence of super-reduced forms of Mn_4−Ca and instead is the result of a very high miss factor, perhaps even more so than that estimated for CP43-R357S by fluorescence techniques (*19*). The absence of oscillations in the pattern of O_2 release in the CP43-R357K mutant made the extraction of Kok parameters using standard algorithms problematic. However, assuming a standard initial S-state distribution similar to the control, an average (homogeneous) miss factor of 46% was obtained for CP43-R357K (Table 2). Although this result is tentative due to its reliance on the assumption on the initial S-state distribution, it fits well with the gradually developing O_2 signal and the absence of discernible oscillations in O_2 yield.

Kinetics of the O_2 signals from isolated membranes deposited as a thin layer on a bare platinum electrode are shown in Figure 4. We observed that the CP43-R357K mutant [Figure 4 (—)] exhibits slightly retarded kinetics in the rise of the O_2 signal compared to the wild type [Figure 4 (- - -)]. The rise time of the O_2 signal depends on the rate constant for O_2 formation during the S_3−[S_4]−S_0 transition and the time for diffusion of oxygen through the intervening buffer to the electrode surface (*50*). The decay of the signal depends on the rise kinetics in a characteristic fashion as discussed previously (*50*), which explains the slower signal decay time observed in the mutant compared to the wild type. Analysis of the rise kinetic of the wild-type signal (*31*, *51*) yields a half-rise time of 0.9 ms, approximating the rate previously estimated for the S_3−[S_4]−S_0 transition, and suggests that the rise kinetic is not limited by diffusion (*31*, *50*−*53*). This rapid rise kinetic reflects minimization of the amount of sample deposited to reduce the diffusion path to the platinum surface and the presence of 250 mM NaCl ensuring a high conductivity and rapid response in the electrode system. Similar analysis with the mutant gives a half-rise time of 4.2 ms, indicating that the CP43-R357K mutation retards the O_2 rise kinetics. The inset of Figure 4 shows an enlargement of the first 4 ms of the O_2 signal. The signals have been normalized to facilitate comparison, and clearly, the mutant signal is noisy compared to that of the wild type. Because of the higher level of noise, it is unclear whether the initial feature seen at the beginning of the mutant signal rise has any biochemical significance or is, more likely, an artifact. No delay between the initiation of the flash ($t = 0$) and the onset in the rise of the O_2 signal is detected in the wild type with this system, yet the mutant appears to have a delay (~250 μs) in the initiation of the signal rise.

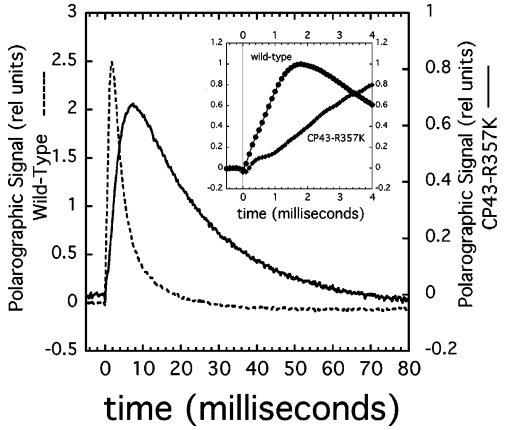

FIGURE 4: Oxygen signals of mutant (—) and wild-type (- - -) membranes. After deposition on the electrode surface, membranes were given a sequence of 20 preflashes and dark-adapted for 10 min, and then 40 measuring flashes were applied and the individual signals compiled from the data set and averaged. Each signal trace represents the average of 35 individual signals. As in Figure 3, the gain on the polarographic signal amplifier was set to be twice as sensitive for the mutant membranes as the wild-type membranes. The exponential rise times of the depicted signals are given in Table 2. Kinetic analysis of the data was performed according to the exponential method described by Jursinic and Dennenberg (*51*). Signals were collected with the analog amplifier high-pass filter set to 2000 Hz and then digitally acquired at a rate of 10 points/ms. A yellow optical filter was used to suppress the photoelectric artifact. The inset shows that the early part of the O_2 signal is enlarged with the signals being normalized to 1.

The very high miss factor during S-state cycling in CP43-R357K deduced from the absence of any oscillatory O_2 yield behavior in dark-adapted samples under flashing light (Figure 3B,D) could, in principle, be due to any one or all of the S-state transitions. Since the single-flash fluorescence decay experiments shown in Figure 2B showed that a single flash in the presence of DCMU produced an apparent S_2 state in a large fraction of the mutant reaction centers, it is possible that a still higher yield of that state could be formed by additional flashes if the quantum yield of the S_1−S_2 transition is low (i.e., has a high miss factor). To test this possibility, essentially the same experiment depicted in Figure 2B was

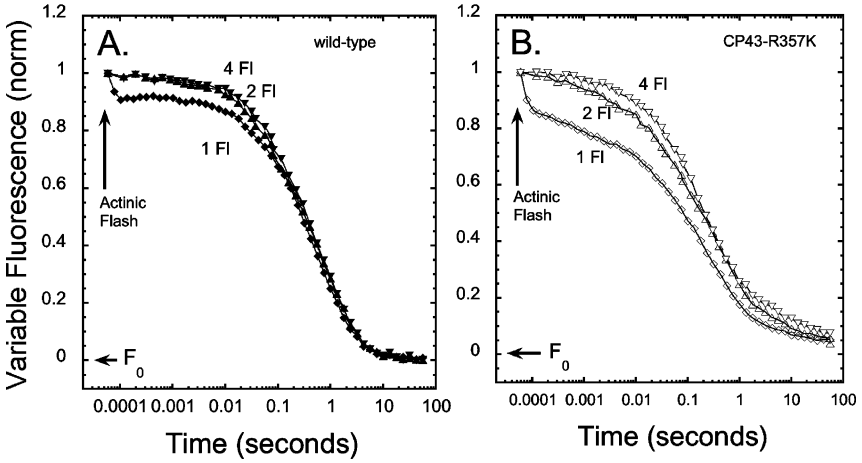

FIGURE 5: Effect of multiple saturating flashes on the accumulation of the S_2 state in the presence of DCMU. Wild-type cells (A) and CP43-R35K cells (B) in the presence of 20 μM DCMU were given a single saturating flash (diamonds), two saturating flashes (triangles), or four saturating flashes (inverted triangles). Multiple flashes were spaced 10 ms apart, and the fluorescence yield was monitored by a train of weak measuring light pulses (eight per decade of time) starting 50 μs after the last saturating actinic flash. Each trace represents the average of three measurements. Variable fluorescence [$F_v = (F_t - F_0)/F_0$] curves are normalized to 1 at the maximal value.

performed, except that a variable number of saturating actinic flashes were given prior to the measurement of fluorescence yield decay (Figure 5). The multiple flashes were given 10 ms apart, which is short compared to the decay of the S_2 state but long enough to allow rapid reaction center charge recombination (Q_A^- with either $P680^+$ or $Y_Z^\bullet$) in centers failing to advance from S_1 to S_2 due to the first flash. Thus, if the quantum yield is low for the S_1-S_2 transition, then application of a second flash should produce a significant increase in the level of the fluorescence component decaying with kinetics corresponding to the decay of the S_2 state. A dramatic change in the shape of the decay curve in response to multiple flashes does not occur in the wild type, although some enhancement of the slowly decaying component corresponding to the decay of the S_2 state does occur (Figure 5A), consistent with the low miss factor associated with the S_1-S_2 transition in wild-type centers (*13*, *54*). As shown for CP43-R357K in Figure 5B, the relative amplitude of the slow phase of decay corresponding to the fraction of PSII centers, tentatively ascribed to the $S_2Q_A^-$ state, was significantly increased at the expense of the fast components, and the signal of the slow component saturated at four flashes. On the basis of the approach to the maximum amplitude of the slow phase, the miss factor for the S_1-S_2 transition is estimated to be ~23%. However, the analysis is complicated by the heterogeneity of fluorescence kinetics, including the emergence of an additional very slow (~10 s) component, probably due to damaged centers. In contrast, the second flash applied to wild-type cells only marginally increased (~6%) the level of the slow component corresponding to the S_2 state, and the subsequent flashes produced no further increase in the magnitude of the slow phase. This high-quantum yield generation of the S_2 state is roughly consistent with the homogeneous (averaged over all S-state transitions) showing a 12% miss factor estimated from the oscillations of O_2 yield (Table 2) for the wild type and previous estimates (*13*, *54*).

DISCUSSION

The CP43-R357K mutation produces a severe defect in the ability of couple charge separation to S-state advancement despite the fact that it permits fairly high levels of assembled PSII. Cells containing the CP43-R357K mutation fail to grow autotrophically and are characterized by a dramatic reduction in O_2 evolving activity (~15% of that of the wild type) despite the fact that mutant cells contained more than 80% of the concentration of charge-separating PSII reaction centers and more than half of these contained photooxidizable Mn. Measurement of O_2 yields using a bare platinum electrode indicated a severe defect in the S-state cycling properties of the mutant H_2O oxidation complexes evidenced by the gradual development of an O_2 signal and the absence of oscillations in O_2 yield under flashing light. These results are best explained by an overall increase in miss factor averaged over all the S states that is clearly very large, with the average miss estimated to be 46% compared to an average miss for the wild type being ~12%. The results are difficult to model using matrix analysis (*41*, *43*), but the presence of super-reduced forms of the complex can be ruled out on the basis of the behavior of the signals in double-flash experiments which actually suggest an enhanced stability of the S_2 state (not shown). The O_2 signal of the mutant was slowed (Figure 4), but not as severely as those of other mutants (*31*, *55*). Perhaps, more interestingly, there appears to be an ~250 μs delay in the initiation of the O_2 signal in the mutant, although signal-to-noise issues and the need for extensive signal averaging mean that this observation needs to be independently confirmed. At the same time, the rise kinetic ($t_{1/2} = 900$ μs) in the wild-type O_2 signal is among the fastest reported, yet the trace provides no evidence of an ~250 μs intermediate as seen by time-resolved X-ray spectroscopy and delayed fluorescence (*24*, *56*). This discrepancy regarding the lack of an ~250 μs intermediate in the wild type may be due to differences in sample source and preparation since the duration of the intermediate appears to be sensitive to these factors (*57*). It is more difficult to reconcile our results with previous rate electrode analysis that also aimed to investigate *Synechocystis* but favored such an intermediate (*53*). In this regard, the kinetics of the rise of the O_2 signal is a function of the length and structure of the diffusion path, the response of the electrode, and the catalytic rate of formation and release of product from the

H_2O oxidase during the $S_3-[S_4]-S_0$ transition (analyzed in ref *50*). Since the observed 900 μs kinetic is close to (even faster than) the rate observed for the transfer of an electron from the Mn complex to $Y_Z^\bullet$, which coincides with dioxygen formation during the S_4-S_0 transition (*24*, *50*−*52*, *58*−*60*), then the kinetics of the electrode signals reported here appear to be rate-limited by the actual dioxygen formation process rather that the subsequent diffusion and response events. Assuming that the ∼250 μs delay observed in the mutant indeed reflects a delay in the initiation of the formation of O_2 from the enzyme, it would then indicate that the primary defect in the mechanism caused by the Arg → Lys substitution is prior to the dioxygen-forming step (S_4-S_0). A strong base is postulated, originally by Krishtalik, to facilitate the deprotonation of active site Mn_4-Ca (*24*−*26*), thereby allowing the otherwise thermodynamically constrained transfer of an electron away from Mn_4-Ca to the oxidized redox active tyrosine radical, $Y_Z^\bullet$, generated by photosynthetic charge separation. Recent proposals suggest the development of positive charge near $Y_Z^\bullet$ [due to constrained proton loss (*61*−*64*)] initiates the deprotonation of CP43-R357, which then has the capacity to abstract a proton from Mn_4-Ca or associated substrate water (*24*, *25*). Our results are consistent with an assignment of CP43-R357 to this function. However, because dioxygen is formed, albeit with impaired quantum efficiency, the substituting lysine or some other base must be capable of substituting for the native arginine in the capacity of abstracting protons assuming that this is, in fact, the normal function of the arginine. While a proton abstracting function for CP43-R357 is an attractive assignment for this residue, more direct approaches will be required to evaluate this hypothesis. Indeed, other chemical groups may perform the requisite proton abstracting role that must occur during water oxidation, and CP43-R357 may instead serve another role within the catalytic site. These possibilities include the binding of an anion such as bicarbonate or Cl^-, which could, in turn, be involved in the proton exit pathway or in positioning substrate water, and at this stage, an allosteric structural role cannot be ruled out.

The multiflash fluorescence experiment depicted in Figure 5 leads us to suggest an increase in the miss factor for the S_1-S_2 transition from 6% in the wild type to 23% in the mutant. In other words, the very high average miss factor (∼43%) during S-state cycling may be due to a defect already apparent during the S_1-S_2 transition. This assessment is based upon the increase in the amplitude of the more slowly decaying 370 ms phase in the mutant that after four flashes bears an uncanny resemblance to the *bona fide* S_2 decay (∼450 ms) phase in the wild type that dominates the kinetics even after the first flash (Figure 5A). The conclusion that an increased miss factor already occurs in the S_1-S_2 transition is rendered tentative due to uncertainties regarding the origin of the fluorescence phases in the mutant. It is also problematic relative to the known properties of the S-state cycle. Notably, findings show (1) under normal conditions the misses are very low for the S_1-S_2 transition and the majority of misses occur during the S_2-S_3 transition and, especially, during the $S_3-[S_4]-S_0$ transition (*65*), (2) various chemical treatments inhibit the higher S-state transitions, but not the S_1-S_2 transition (e.g., refs *66* and *67*), and (3) the S_1-S_2 transition is much less pH-dependent than the transitions to higher S states (*54*). On the other hand, there is precedent for mutations in *Synechocystis* PSII being inhibited S_1-S_2 transitions. Mutation of histidine 332 of the D1 protein results in an inhibition of the S_1-S_2 transition, with the glutamate substitution (D1-H332E) being most severe and shown to exhibit a very low quantum yield for formation of the S_2 multiline EPR signal (*68*, *69*). Examination of the fluorescence kinetics of this mutant, as well as other D1-H332 substitutions, revealed characteristics not unlike those observed here: multiple flashes were required for the complete accumulation of fluorescence decay phases attributed to $Q_A^-S_2$ recombination (*44*). On the basis of these considerations, the less efficient photoaccumulation of the slow fluorescence decay phase, while suggestive, is only tentatively attributed to an impaired quantum yield of the S_1-S_2 transition in the mutant, and thus, this issue awaits a more definitive analysis. However, the possibility that the S_1-S_2 transition may also have a high miss factor suggests that if this residue does serve a role in facilitating PCET in the higher S states, then this function may be in operation in the lower S states and, perhaps, even during the assembly of Mn_4-Ca given its proximity to the high-affinity site ligand, D1-Asp170.

NOTE ADDED AFTER ASAP PUBLICATION

This paper was published ASAP on October 4, 2007, with a minor text error in the abstract. The correct version was published on October 5, 2007.

REFERENCES

1. Joliot, P., Barbieri, G., and Chabaud, R. (1969) Un nouveau modele des centres photochimique du systeme II, *Photochem. Photobiol. 10*, 309−329.
2. Kok, B., Forbush, B., and McGloin, M. (1970) Cooperation of charges in photosynthetic oxygen evolution: I. A linear four step mechanism, *Photochem. Photobiol. 11*, 457−475.
3. Goussias, C., Boussac, A., and Rutherford, A. W. (2002) Photosystem II and photosynthetic oxidation of water: An overview, *Philos. Trans. R. Soc. London, Ser. B 357*, 1369−1381.
4. Sauer, K., Yano, J., and Yachandra, V. K. (2005) X-ray spectroscopy of the Mn_4Ca cluster in the water-oxidation complex of Photosystem II, *Photosynth. Res. 85*, 73−86.
5. Hillier, W., and Messinger, J. (2005) Mechanism of Photosynthetic Oxygen Production, in *Photosystem II: The Light-Driven Water: Plastoquinone Oxidoreductase* (Wydrzynski, T., and Satoh, K., Eds.) pp 567−608, Springer, Dordrecht, The Netherlands.
6. McEvoy, J. P., and Brudvig, G. W. (2006) Water-splitting chemistry of photosystem II, *Chem. Rev. 106*, 4455−4483.
7. Ferreira, K. N., Iverson, T. M., Maghlaoui, K., Barber, J., and Iwata, S. (2004) Architecture of the photosynthetic oxygen-evolving center, *Science 303*, 1831−1838.
8. Kamiya, N., and Shen, J. R. (2003) Crystal structure of oxygen-evolving photosystem II from *Thermosynechococcus vulcanus* at 3.7-Å resolution, *Proc. Natl. Acad. Sci. U.S.A. 100*, 98−103.
9. Loll, B., Kern, J., Saenger, W., Zouni, A., and Biesiadka, J. (2005) Towards complete cofactor arrangement in the 3.0 Å resolution structure of photosystem II, *Nature 438*, 1040−1044.
10. Zouni, A., Witt, H. T., Kern, J., Fromme, P., Krauss, N., Saenger, W., and Orth, P. (2001) Crystal structure of photosystem II from *Synechococcus elongatus* at 3.8 Å resolution, *Nature 409*, 739−743.
11. Yano, J., Kern, J., Irrgang, K. D., Latimer, M. J., Bergmann, U., Glatzel, P., Pushkar, Y., Biesiadka, J., Loll, B., Sauer, K., Messinger, J., Zouni, A., and Yachandra, V. K. (2005) X-ray damage to the Mn_4Ca complex in single crystals of photosystem II: A case study for metalloprotein crystallography, *Proc. Natl. Acad. Sci. U.S.A. 102*, 12047−12052.
12. Dau, H., Liebisch, P., and Haumann, M. (2004) The structure of the manganese complex of Photosystem II in its dark-stable S-1-state-EXAFS results in relation to recent crystallographic data, *Phys. Chem. Chem. Phys. 6*, 4781−4792.

13. Grabolle, M., Haumann, M., Muller, C., Liebisch, P., and Dau, H. (2006) Rapid loss of structural motifs in the manganese complex of oxygenic photosynthesis by X-ray irradiation at 10−300 K, *J. Biol. Chem. 281*, 4580−4588.
14. Diner, B. A., and Rappaport, F. (2002) Structure, Dynamics, and Energetics of the Primary Photochemistry of Photosystem II of Oxygenic Photosynthesis, *Annu. Rev. Plant Physiol. Plant Mol. Biol. 53*, 551−580.
15. Babcock, G. T., Barry, B. A., Debus, R. J., Hoganson, C. W., Atamian, M., McIntosh, L., Sitole, I., and Yocum, C. F. (1989) Water oxidation in photosystem II: From radical chemistry to multielectron chemistry, *Biochemistry 28*, 9557−9565.
16. Knoepfle, N., Bricker, T. M., and Putnam-Evans, C. (1999) Site-directed mutagenesis of basic arginine residues 305 and 342 in the CP 43 protein of photosystem II affects oxygen-evolving activity in *Synechocystis* 6803, *Biochemistry 38*, 1582−1588.
17. Rosenberg, C., Christian, J., Bricker, T. M., and Putnam-Evans, C. (1999) Site-directed mutagenesis of glutamate residues in the large extrinsic loop of the photosystem II protein CP 43 affects oxygen-evolving activity and PS II assembly *Biochemistry 38*, 15994−16000.
18. Bricker, T. M. (1990) The structure and function of CPa-1 and CPa2 in photosystem II, *Photosynth. Res. 24*, 1−13.
19. Ananyev, G., Nguyen, T., Putnam-Evans, C., and Dismukes, G. C. (2005) Mutagenesis of CP43-arginine-357 to serine reveals new evidence for (bi)carbonate functioning in the water oxidizing complex of Photosystem II, *Photochem. Photobiol. Sci. 4*, 991−998.
20. Klimov, V. V., Allakhverdiev, S. I., Feyziev, Ya. M., and Baranov, S. V. (1995) Bicarbonate requirement for the donor side of photosystem II, *FEBS Lett. 3635*, 251−255.
21. Baranov, S. V., Ananyev, G. M., Klimov, V. V., and Dismukes, G. C. (2000) Bicarbonate accelerates assembly of the inorganic core of the water-oxidizing complex in manganese-depleted photosystem II: A proposed biogeochemical role for atmospheric carbon dioxide in oxygenic photosynthesis, *Biochemistry 39*, 6060−6065.
22. Lambert, L. A., Perri, H., Halbrooks, P. J., and Mason, A. B. (2005) Evolution of the transferrin family: Conservation of residues associated with iron and anion binding, *Comp. Biochem. Physiol. 142*, 129−141.
23. Haumann, M., Barra, M., Loja, P., Loscher, S., Krivanek, R., Grundmeier, A., Andreasson, L. E., and Dau, H. (2006) Bromide does not bind to the Mn_4Ca complex in its S-1 state in Cl-depleted and Br^--reconstituted oxygen-evolving photosystem II: Evidence from X-ray absorption spectroscopy at the BrK-edge, *Biochemistry 45*, 13101−13107.
24. Haumann, M., Liebisch, P., Muller, C., Barra, M., Grabolle, M., and Dau, H. (2005) Photosynthetic O-2 formation tracked by time-resolved X-ray experiments, *Science 310*, 1019−1021.
25. McEvoy, J. P., and Brudvig, G. W. (2004) Structure-based mechanism of photosynthetic water oxidation, *Phys. Chem. Chem. Phys. 6*, 4754−4763.
26. Krishtalik, L. I. (1986) Energetics of Multielectron Reactions: Photosynthetic Oxygen Evolution, *Biochim. Biophys. Acta 849*, 162−171.
27. Vrettos, J. S., Limburg, J., and Brudvig, G. W. (2001) Mechanism of photosynthetic water oxidation: Combining biophysical studies of photosystem II with inorganic model chemistry, *Biochim. Biophys. Acta 1503*, 229−245.
28. Zak, O., Aisen, P., Crawley, J. B., Joannou, C. L., Patel, K. J., Rafiq, M., and Evans, R. W. (1995) Iron release from recombinant N-lobe and mutants of human transferrin, *Biochemistry 34*, 14428−14434.
29. Burnap, R., Koike, H., Sotiropoulou, G., and Sherman, L. A. I. Y. (1989) Oxygen evolving membranes and particles from the transformable cyanobhacterium *Synechocystis* sp. PCC6803, *Photosynth. Res. 22*, 123−130.
30. Krishtalik, L. I., Tae, G. S., Cherepanov, D. A., and Cramer, W. A. (1993) The redox properties of cytochromes b imposed by the membrane electrostatic environment, *Biophys. J. 65*, 184−195.
31. Qian, M., Dao, L., Debus, R. J., and Burnap, R. L. (1999) Impact of mutations within the putative Ca^{2+}-binding lumenal interhelical a-b loop of the photosystem II D1 protein on the kinetics of photoactivation and H_2O-oxidation in *Synechocystis* sp. PCC6803, *Biochemistry 38*, 6070−6081.
32. Strickler, M. A., Walker, L. M., Hillier, W., and Debus, R. J. (2005) Evidence from biosynthetically incorporated strontium and FTIR difference spectroscopy that the C-terminus of the D1 polypeptide of photosystem II does not ligate calcium, *Biochemistry 44*, 8571−8577.
33. Tang, X. S., and Diner, B. A. (1994) Biochemical and spectroscopic characterization of a new oxygen evolving photosystem II core complex from the cyanobacterium *Synechocystis* PCC 6803, *Biochemistry 33*, 4594−4603.
34. Williams, J. G. K. (1988) Construction of specific mutations in Photosystem II photosynthetic reaction center by genetic engineering methods in *Synechocystis* 6803, *Methods Enzymol. 167*, 766−778.
35. Debus, R. J. (2001) Amino acid residues that modulate the properties of tyrosine Y_Z and the manganese cluster in the water oxidizing complex of photosystem II, *Biochim. Biophys. Acta 1503*, 164−186.
36. Goldfarb, N., Knoepfle, N., and Putnam-Evans, C. (1997) Construction of a psb C deletion strain in *Synechocystis* 6803, *SAAS Bull. Biochem. Biotechnol. 10*, 1−6.
37. Bricker, T. M., Morvant, J., Masri, N., Sutton, H. M., and Frankel, L. K. (1998) Isolation of a highly active photosystem II preparation from *Synechocystis* 6803 using a histidine-tagged mutant of CP 47, *Biochim. Biophys. Acta 1409*, 50−57.
38. Li, Z., Bricker, T. M., and Burnap, R. (2000) Kinetic characterization of His-tagged CP47 photosystem II in *Synechocystis* sp. PCC6803, *Biochim. Biophys. Acta 1460*, 384−389.
39. Nixon, P. J., and Diner, B. A. (1992) Aspartate 170 of the photosystem II reaction center polypeptide D1 is involved in the assembly of the oxygen evolving manganese cluster, *Biochemistry 31*, 942−948.
40. Li, Z. L., and Burnap, R. L. (2002) Mutations of basic arginine residue 334 in the D1 protein of Photosystem II lead to unusual S-2 state properties in *Synechocystis* sp PCC 6803, *Photosynth. Res. 72*, 191−201.
41. Lavorel, J. (1976) Matrix analysis of the oxygen evolving system of photosynthesis, *J. Theor. Biol. 57*, 171−185.
42. Meunier, P. C., Burnap, R. L., and Sherman, L. A. (1995) Interactions of the photosynthetic and respiratory electron transport chains producing slow apparent O_2 releases under flashing light in *Synechocystis* sp. PCC 6803, *Photosynth. Res. 45*, 31−40.
43. Meunier, P. C., Burnap, R. L., and Sherman, L. A. (1995) Modelling of the S-state mechanism and Photosystem II manganese photoactivation in cyanobacteria, *Photosynth. Res. 47*, 61−76.
44. Allahverdiyeva, Y., Deak, Z., Szilard, A., Diner, B. A., Nixon, P. J., and Vass, I. (2004) The function of D1-H332 in Photosystem II electron transport studied by thermoluminescence and chlorophyll fluorescence in site-directed mutants of *Synechocystis* 6803, *Eur. J. Biochem. 271*, 3523−3532.
45. Rappaport, F., Guergova-Kuras, M., Nixon, P. J., Diner, B. A., and Lavergne, J. (2002) Kinetics and Pathways of Charge Recombination in Photosystem II, *Biochemistry 41*, 8518−8527.
46. Chu, H.-A., Nguyen, A. P., and Debus, R. A. (1994) Site-directed mutagenesis of photosynthetic oxygen evolution: Instability or inefficient assembly of the manganese cluster *in vivo*, *Biochemistry 33*, 6137−6149.
47. Chu, H. A., Nguyen, A. P., and Debus, R. J. (1995) Amino acid residues that influence the binding of manganese or calcium to photosystem II. 1. The lumenal interhelical domains of the D1 polypeptide, *Biochemistry 34*, 5839−5858.
48. Bouges-Bocquet, B. (1973) Limiting steps in photosystem II and water decomposition in *Chlorella* and spinach chloroplasts, *Biochim. Biophys. Acta 292*, 772−785.
49. Li, Z.-L., and Burnap, R. L. (2002) Mutations of Basic Arginine Residue 334 in the D1 Protein of Photosystem II Lead to An Unusual S2 State Decay in *Synechocystis* sp. PCC6803, *Photosynth. Res. 72*, 191−202.
50. Lavorel, J. (1992) Determination of the photosynthetic oxygen release time by amperometry, *Biochim. Biophys. Acta 1101*, 33−40.
51. Jursinic, P. A., and Dennenberg, R. J. (1990) Oxygen release time in leaf discs and thylakoids of peas and Photosystem II membrane fragments of spinach, *Biochim. Biophys. Acta 1020*, 195−206.
52. Meunier, P. C., and Popovic, R. (1991) The time for oxygen release in photosynthesis: Reconciliation of flash polarography with other measurement techniques, *Photosynth. Res. 28*, 33−39.

53. Clausen, J., Debus, R. J., and Junge, W. (2004) Time-resolved oxygen production by PSII: Chasing chemical intermediates, *Biochim. Biophys. Acta 1655*, 184−194.
54. Bernat, G., Morvaridi, F., Feyziyev, Y., and Styring, S. (2002) pH dependence of the four individual transitions in the catalytic S-cycle during photosynthetic oxygen evolution, *Biochemistry 41*, 5830−5843.
55. Hundelt, M., Hays, A. M., Debus, R. J., and Junge, W. (1998) Oxygenic photosystem II: The mutation D1-D61N in *Synechocystis* sp. PCC 6803 retards S-state transitions without affecting electron transfer from YZ to $P680^+$, *Biochemistry 37*, 14450−14456.
56. Buchta, J., Grabolle, M., and Dau, H. (2007) Photosynthetic dioxygen formation studied by time-resolved delayed fluorescence measurements: Method, rationale, and results on the activation energy of dioxygen formation, *Biochim. Biophys. Acta 1767*, 565−574.
57. Razeghifard, M. R., and Pace, R. J. (1999) EPR kinetic studies of oxygen release in thylakoids and PSII membranes: A kinetic intermediate in the S3 to S0 transition, *Biochemistry 38*, 1252−1257.
58. Babcock, G. T., Blankenship, R. E., and Sauer, K. (1976) Reaction kinetics for positive charge accumulation on the water side of chloroplast photosystem II, *FEBS Lett. 61*, 286−289.
59. Razeghifard, M. R., Klughammer, C., and Pace, R. J. (1997) Electron paramagnetic resonance kinetic studies of the S states in spinach thylakoids, *Biochemistry 36*, 86−92.
60. Razeghifard, M. R., Wydrzynski, T., Pace, R. J., and Burnap, R. L. (1997) $Y_Z^\bullet$ reduction kinetics in the absence of the manganese-stabilizing protein of photosystem II, *Biochemistry 36*, 14474−14478.
61. Haumann, M., Mulkidjanian, A., and Junge, W. (1999) Tyrosine-Z in oxygen-evolving photosystem II: A hydrogen-bonded tyrosinate, *Biochemistry 38*, 1258−1267.
62. Eckert, H. J., Wiese, N., Bernarding, J., Eichler, H. J., and Renger, G. (1988) Analysis of the electron transfer from Pheo- to QA in PS II membrane fragments from spinach by time resolved 325 nm absorption changes in the picosecond domain, *FEBS Lett. 240*, 153−158.
63. Ahlbrink, R., Haumann, M., Cherepanov, D., Bogershausen, O., Mulkidjanian, A., and Junge, W. (1998) Function of tyrosine Z in water oxidation by photosystem II: Electrostatical promotor instead of hydrogen abstractor, *Biochemistry 37*, 1131−1142.
64. Rappaport, F., and Lavergne, J. (1997) Charge recombination and proton transfer in manganese depleted photosystem II, *Biochemistry 36*, 15294−15302.
65. Grabolle, M., and Dau, H. (2007) Efficiency and role of loss processes in light-driven water oxidation by PSII, *Physiol. Plant. 131*, 50−63.
66. Wincencjusz, H., van Gorkom, H. J., and Yocum, C. F. (1997) The photosynthetic oxygen evolving complex requires chloride for its redox state S2 → S3 and S3 → S0 transitions but not for S0 → S1 or S1 → S2 transitions, *Biochemistry 36*, 3663 3670.
67. Wincencjusz, H., Yocum, C. F., and van Gorkom, H. J. (1999) Activating anions that replace Cl^- in the O_2-evolving complex of photosystem II slow the kinetics of the terminal step in water oxidation and destabilize the S2 and S3 states, *Biochemistry 38*, 3719−3725.
68. Chu, H. A., Nguyen, A. P., and Debus, R. J. (1995) Amino acid residues that influence the binding of manganese or calcium to photosystem II. 2. The carboxy terminal domain of the D1 polypeptide, *Biochemistry 34*, 5859−5882.
69. Debus, R. J., Campbell, K. A., Gregor, W., Li, Z. L., Burnap, R. L., and Britt, R. D. (2001) Does histidine 332 of the D1 polypeptide ligate the manganese cluster in photosystem II? An electron spin echo envelope modulation study, *Biochemistry 40*, 3690−3699.

BI701387B